Research Article

Impact of Wind Power Forecasting Error Bias on the Economic Operation of Autonomous Power Systems

Antonis G. Tsikalakis* and Nikos D. Hatziargyriou, School of Electrical and Computer Engineering, National Technical University of Athens, Zografou 15780, Greece
Yiannis A. Katsigiannis and Pavlos S. Georgilakis, Department of Production Engineering and Management, Technical University of Crete, Chania 73100, Greece

Many efforts have been presented in the literature for wind power forecasting in power systems and few of them have been used for autonomous power systems. In addition, some recent studies have evaluated the impact on the operation of power systems and energy markets that the improvement of wind power forecasting can have. In this paper, the value of the information provided to the operators of autonomous power systems about forecasting errors is studied. This information may vary significantly, e.g. it can be only the normalized mean absolute error of the forecast, or a probability density function of the errors for various levels of forecasted wind power, which can be provided either during the evaluation phase of the wind power forecasting tool or by online uncertainty estimators. This paper studies the impact of the level of detail provided about wind power forecasting accuracy for various levels of load and wind power production. The proposed analysis, when applied to the autonomous power system of Crete, shows significant changes among the various levels of information provided, not only in the operating cost but also in the wind power curtailment. Copyright © 2008 John Wiley & Sons, Ltd.

Introduction

Many efforts have been presented in the technical literature for wind power forecasting (wpf) in power systems,[1–7] but few of them have been used for autonomous power systems.[7,8] Recent studies[9–14] have shown that improving wpf has significant economic savings for both utilities and the wind park owners participating in the energy market. The impact of different forecasting errors for different utilities and wind power production levels has been studied, and the presented results show that the economic benefits for utilities are increased as forecasting accuracy is increased, and even for low wind power production, this can be significant.[10] A review of studies on the impact of wind power integration in some US utilities has indicated the significance of wind power forecasting in reducing the imbalance costs and the spinning reserve requirements.[11] For

example, in December 2000, Southern California Edison saved $2 million in imbalance costs by improving its wpf.[12] A similar study deals with the importance of short-term wind power prediction in the participation of wind power in electricity markets in Spain[13] and other European countries.[14]

Significant progress has been also made in the uncertainty assessment of wind power forecasts and their application in wind power integration in electricity markets,[15] using meteorological ensembles,[16,17] physical considerations[18] or statistical methods.[3,19–21] As an example, local quantile regression has been applied to optimize the income of a wind power producer by identifying which quantile of the probability distribution for wind power production should be used when bidding in the open market,[22] also stressing how the prediction uncertainty estimation can help in minimizing imbalance costs. The re-sampling method[23] has been also used to make uncertainty estimation and to identify the confidence intervals of a wpf tool.

Effective wind power forecasting is very important for the secure and economic operation of autonomous power systems with increased wind power penetration. In such systems, because of the lack of interconnection to other power systems, spinning reserve requirements are increased to account for the uncertainties in load and wind power predictions or contingencies. This leads to excessive spinning reserve and increase of operating costs. Moreover, such power systems present low minimum-to-maximum demand ratio and significantly larger frequency deviations compared with interconnected power systems. The technical minima of the installed thermal units often impose limitations in wind power integration, imposing wind power curtailment in order to avoid technical limits violations. The higher the uncertainty in the estimation of load and wind, the higher the expected wind power curtailment, especially in power systems with slow response units. Advanced control software tools, like MORE CARE,[8] have been developed to aid island system operators by incorporating load and renewable energy sources forecasting functions,[7] unit commitment, economic dispatch (ED) and online dynamic security assessment modules.

Taking into account the special features of autonomous power systems, it would be highly desirable to have a methodology to quantify the expected forecasting errors and to use the information provided by the forecasting tools more efficiently.

In this paper, the value of the information on wind power forecasting errors, to account for the uncertainty in wind power forecasting, is studied. Such information can be derived from the results of an off-line evaluation or from the suppliers of the forecasting tool, e.g. confidence interval and uncertainty estimators. A methodology for exploiting information as little as normalized mean absolute error (NMAE) to a probability density function (pdf) of the wpf error for various levels of forecasted wind power, combined with the load forecasting error, is described. According to this methodology, using the calculated percentiles, the operators can derive confidence intervals for the uncertainty of the equivalent load to be dispatched to the thermal units. This is taken into account for the spinning reserve and wind power curtailment calculations. The method is applied to the typical autonomous power system of Crete using an actual load and wind power data and their forecasts. The obtained results are presented and discussed and conclusions are drawn.

Proposed Methodology

The load expected to be dispatched to the thermal units is $load(t)$–$WP(t)$, where $load(t)$ is the output of the load forecasting tool and $WP(t)$ is the output of the wpf tool. The uncertainty in the load to be dispatched to the thermal units at each time interval, t, namely $lw_e(t)$, comes from load and wind power forecasting error, $l_e(t)$ and $w_e(t)$, respectively.

$$lw_e(t) = l_e(t) - w_e(t) \tag{1}$$

The following three steps are followed:

• Convolution of the forecasting errors probability density functions.
• Derivation of confidence intervals in q and p percentiles for the convolution results.
• Economic scheduling.

It is assumed that both forecasting errors are statistically independent random variables[11] and thus the probability density functions of $l_e(t)$ and $w_e(t)$ can be convoluted to produce the $lw_e(t)$ probability density function.

Having calculated the $lw_e(t)$ pdf, confidence intervals for the expected uncertainty of the load to be distributed to the thermal units can be derived, expressed as the interval between p and q percentiles.

The q percentile, $perc[q, lw_e(t)]$, of the cumulative distribution function (cdf), $F_{lwe(t)}[lw_e(t)]$, of the $lw_e(t)$ pdf is the solution of the following equation:

$$F_{lwe(t)}[lw_e(t)] = q \qquad (2)$$

The solution of equation (2) depends on the pdf that is derived according to the available information, as presented next. According to the desired confidence interval, the economic scheduling functions identify which units operate, their production and if there is any need for wind power curtailment.

Normalized prediction errors have been considered in this paper for both load and wind power forecasting, as described in equation (3). Thus, the errors take into account any loading or installed wind power capacity of the power system under study. In equation (3), P_f stands for the forecasted value, P_a for the actual value and P_i stands for the reference value. For the case of load forecasting, the reference value is the installed wind power capacity. Negative values of e_r mean overestimation of the actual value, whereas positive values mean underestimation.

$$e_r = \left(\frac{P_a - P_f}{P_i} \right) \cdot 100\% \qquad (3)$$

Any prediction error, as shown in equation (4), can be decomposed into a systematic error μ_e, i.e. the bias and a random error ξ_e, considered here as a zero mean random variable.

$$e_r = \mu_e + \xi_e \qquad (4)$$

The suppliers of load and wind power forecasting tools provide end-users with information at least about the *NMAE* as described in equation (5):[24]

$$NMAE = \frac{1}{pds} \cdot \sum_{i=1}^{pds} |e_r| \qquad (5)$$

where *pds* states the number of considered evaluation periods.

The *NMAE* index provides very little information about the forecasting errors. Even if two wind power forecasting tools present the same *NMAE*, the one may more often overestimate the wind power, whereas the other may more often underestimate it.

Statistical analysis of the error e_r provided by equation (4) increases the available information to the operators of a power system, as discussed next. Table I presents the possible levels of available information about wpf error.

In Case 1, considered as the base case, only *NMAE* is known. Symmetrical and unbiased forecasting errors are assumed meaning $\mu_e = 0$, and ξ_e is represented by Normal pdf as shown in Figure 1.

Case 2 assumes that, in addition to *NMAE*, the percentage of underestimation and overestimation errors is known. In the following, a mathematical description of the combination of the information about frequency

Table I. Cases of available information on wind power forecasting errors

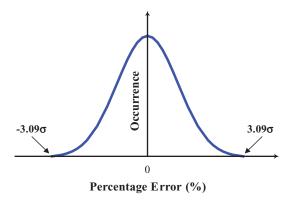| Case	Available information
1	Only *NMAE* is known, 50% overestimation and 50% underestimation error is assumed as well as Gaussian distribution of errors
2	Occurrence of overestimation and underestimation error in addition to *NMAE*
3	Distribution of wpf errors
4	Distribution of wpf error grouped for various wind power forecasting outputs

Figure 1. Plot of the pdf considered for forecasting error when only NMAE is known

of overestimation errors with the normalized bias (NBIAS) of the forecasting errors is provided. Derivation of the $lw_e(t)$ pdf is common for Cases 1 and 2, based on convolution techniques for Normal pdfs.

For Cases 3 and 4, a discrete pdf of the wpf errors is available. In Case 4, this pdf is different for high or low wind power forecasted. This consideration is accordance with the recent progress in wpf tools that can provide with uncertainty estimates given by probabilistic forecasts.[2,3,7,15,22,23,25]

Calculating Forecasting Error Parameters when NMAE and Frequency of Underestimation and Overestimation Errors are Known

The *NMAE* of a forecasting error e_r is mathematically equivalent to the expected value of $|e_r|$. The random error in equation (4), ξ_e, is assumed to follow a Normal pdf N(ξ_e, 0, σ) with zero mean value and standard deviation σ. Based on this assumption it is proven[26] that e_r, which is a linear function of ξ_e, follows N(ξ_e, 0, σ). In equations (7) and (8), the parameters *a* and *b* denote the frequency of overestimation and underestimation forecasting errors, respectively:

$$\int_{-\infty}^{\infty} |e_r| \cdot N(e_r, \mu_e, \sigma) \cdot de_r = NMAE \tag{6}$$

$$\int_{-\infty}^{0} N(e_r, \mu_e, \sigma) \cdot de_r = a \tag{7}$$

Equation (6) is transformed into equation (8), using the integral calculations described in the Appendix.

$$\mu_e \cdot (b-a) + 2 \cdot \frac{\sigma}{\sqrt{2\pi}} \cdot \exp\left[-\frac{1}{2} \cdot \left(-\frac{\mu_e}{\sigma}\right)^2\right] = NMAE \tag{8}$$

Using the central limit theorem and the tables of the Normal cdf, the $F_N(x, 0, 1)$, μ_e/σ ratio is calculated for the specific value of the second part of equation (7). If the NBIAS, which is equal to μ_e, is known, σ is straight-forwardly calculated, otherwise the solution of the system of equations (7) and (8) provides the parameters μ_e and σ.

Cases 1 and 2

Without any further information about the frequency of overestimation or underestimation errors of a forecasting tool, a 50% probability to overestimate the actual value and 50% probability to underestimate it, can be simply assumed. A further assumption is that the forecasting error follows a Normal pdf with zero mean and standard deviation σ, as calculated by equation (8). In such a case, the system of equations (6) and (7) has the following solution representing Case 1:

$$\sigma = \frac{NMAE}{2} \cdot \sqrt{2 \cdot \pi} \quad \text{and} \quad \mu_e = 0 \tag{9}$$

Nevertheless, the forecasting errors are almost never symmetrical.[27,28] Since the *NMAE* does not provide any information about asymmetry, the frequencies of overestimation and underestimation are essential, as in Case 2. For different frequencies of overestimation and underestimation, different values of σ and μ_e can be calculated for the same *NMAE*, as Table II presents.

The pdf for $lw_e(t)$ is the result of the convolution of the pdfs for $l_e(t)$ and $w_e(t)$ and for continuous variables is given by equation (10):

$$f_{lw_e(t)}[lw_e(t)] = \int_{-\infty}^{+\infty} f_{l_e(t)}[l_e(t) - x] \cdot f_{w_e(t)}[w_e(t)]dx \tag{10}$$

The convolution of two random variables following Normal pdf is, according to the probability theory, a Normal pdf $N(x, \mu, \sigma)$ with the following parameters:[28]

- Mean value, μ, the summation of the mean values of the two random variables, $\mu = \mu_1 + \mu_2$.
- Standard deviation, σ, calculated as $\sigma^2 = \sigma_1^2 + \sigma_1^2$ where σ_1 and σ_2 are the standard deviation of each random variable.

The mean value and the standard deviation for $lw_e(t)$ are provided by equations (11) and (12):

$$\mu(t) = \mu_{le(t)}(t) \cdot load(t) + \mu_{We(t)}(t) \cdot InsCap \tag{11}$$

$$\sigma^2(t) = [\sigma_{le(t)}(t) \cdot load(t)]^2 + [\sigma_{We(t)}(t) \cdot InsCap]^2 \tag{12}$$

InsCap denotes wind power installed capacity; $\mu_{le(t)}(t)$ and $\mu_{we(t)}(t)$ stands for the mean values and $\sigma_{le(t)}(t)$ and $\sigma_{we(t)}(t)$ represents the standard deviations for the forecasting errors of load and wind power, respectively.

Having calculated the parameters of the Normal pdf, the p and q percentiles for $lw_e(t)$ can be estimated using Normal cdf tables at the corresponding points k_q and k_p, respectively, as described by equations (13) and (14).

$$perc[q, lw_e(t)] = \mu(t) + k_q \cdot \sigma(t) \tag{13}$$

$$perc[p, lw_e(t)] = \mu(t) + k_p \cdot \sigma(t) \tag{14}$$

The wind power production cannot exceed the operation limits $[0, InsCap]$. This means that inequalities (15) and (16) should be valid, when calculating the required percentiles of the wpf error and the wind power forecasted value, $WP(t)$.

$$WP(t) + perc[1 - q, w_e(t)] \le InsCap \Leftrightarrow perc[1 - q, w_e(t)] \le InsCap - WP(t) \tag{15}$$

$$WP(t) + perc[1 - q, w_e(t)] \ge 0 \Leftrightarrow perc[1 - q, w_e(t)] \ge -WP(t) \tag{16}$$

Table II. Wind power underestimation and overestimation scenarios for Case 2

a (%)	b (%)	μ_e (normalized bias)	σ
50	50	0	0.177
30	70	−0.082	0.156
35	65	−0.063	0.165
40	60	−0.043	0.171
45	55	−0.022	0.175
55	45	0.022	0.175
60	40	0.0433	0.171
65	35	0.063	0.165
70	30	0.082	0.156

In order to overcome violation of equations (15) and (16), it is checked whether the probability of violating the limits of wind power production [0, *InsCap*], is higher than *p*% and (1–*q*)%, respectively. These values are chosen in accordance with the percentiles of $lw_e(t)$, equations (13) and (14), to ensure that the impact of such a violation is negligible.

If any probability is higher than these determined values, wpf error pdf is represented by a mixed discrete and continuous pdf, like the one depicted in Figure 2. The mathematical description of the modified pdf that does not violate inequality (15) is provided by equation (17), and the discrete impulse is at the *InsCap–WP(t)* point. The modified pdf, in order not to violate zero production, inequality (16), has mathematical formulation similar to equation (17) and the discrete impulse is at the −*WP(t)* point. The probability of having $w_e(t)$ values leading to violation of the limits should be zero. Therefore, the discrete impulse at the above discussed points is the one that sums up the rest of the points of the Normal pdf that should be curtailed, assuring that the integral of $f_{w_e(t)}[w_e(t)]$ is equal to one.

$$f_{w_e(t)}(w_e(t)) = \begin{cases} N\left(w_e(t), \mu_{w_e(t)}(t)\cdot InsCap, [\sigma_{w_e(t)}(t)\cdot InsCap]^2\right) & \text{if } w_e(t) < InsCap - WP(t) \\ 1 - F_N[InsCap - WP(t), \mu_{w_e(t)}(t)]\cdot InsCap, [\sigma_{w_e(t)}(t)\cdot InsCap]^2 & \text{if } w_e(t) = InsCap - WP(t) \\ 0 & \text{if } w_e(t) = InsCap - WP(t) \end{cases} \quad (17)$$

In order to derive the required percentile points for $lw_e(t)$, discrete pdfs for both the updated wpf error pdf of Figure 2 and the load forecasting error pdf are derived, and these two discrete pdfs are convoluted. Then for the inequality that is expected to be violated, the required percentile for $lw_e(t)$ is taken by sorting the outputs of the discrete pdf points. For instance, if inequality (15) is violated, the *p* percentile of $lw_e(t)$ is found using the discrete pdf. The *q* percentile can be found using equation (13).

Case 3

In most cases, the wpf errors do not follow Normal distributions.[27,28] Operators might know the occurrence of underestimation and overestimation errors, but they do not know how often extreme errors may occur. To cope with this, the pdf of the forecasting errors can be derived by grouping the e_r values to provide a discrete function, such as the one shown in Figure 3, and mathematically formulated by the Dirac function δ, as in equation (18):

$$f_{we(t)}[w_e(t)] = \sum_{k=1}^{m} G_k \cdot \delta[w_e(t) - H_k] \quad (18)$$

where *m* is the number of impulses, G_k is the value of each bin and H_k the bin of wpf error. If we assume that $l_e(t)$ follows a Normal pdf N(*x*, μ_1, σ_1), then $lw_e(t)$ is obtained by a convolution of a discrete pdf and a Gaussian pdf. This convolution is obtained by equation (19), as explained in Miranda, Cerqueira and Monteiro:[27]
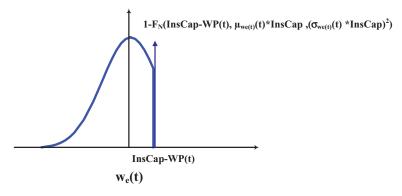

Figure 2. Combined discrete and Normal pdf considered for Case 2 to avoid violation of wind power operating limits
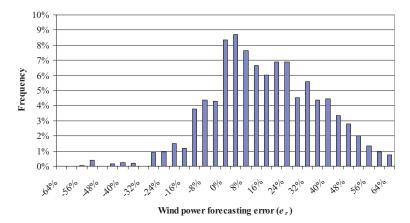
Figure 3. Typical distribution of wind power forecasting error after off-line evaluation

$$f_w(w) = f_N(x_N) \cdot f_D(x_D) = \sum_{k=1}^{m} \frac{G_k}{\sigma_N \sqrt{2\pi}} \cdot \exp\left[-\frac{(w - \mu_{wk})^2}{2 \cdot \sigma_N^2}\right] \tag{19}$$

where σ_N is the standard deviation of the Normal pdf, load forecasting error in our case, and the mean value of the new pdf is given by $\mu_{wk} = \mu_N + H_k$, where μ_N is the mean value of the Gaussian pdf.

In such a case, estimating the required percentile requires the solution of equation (20):

$$G_1 \cdot F_x(x) + G_2 \cdot F_x(x + k_1 \cdot \sigma) = p\% \tag{20}$$

where $H_1 = 0$, $H_2 = k_1 \cdot \sigma$ and $G_1 + G_2 = 1$ are all considered known. The number of adders in equation (20) is equal to m. The solution of such equation is not straightforward, and, as the number of adders increases more than two as in this example, the solution is getting more difficult. Thus, the user-defined confidence interval for $lw_e(t)$ is calculated by discretizing the corresponding cdf and taking the corresponding percentile points.

Case 4

Normally, for certain wind power values, some types of forecasting errors are expected to be very rare, e.g. high overestimation error during a low wind speed period, or high underestimation error during a high wind speed period.[29] Operators are much more concerned about wpf errors during high wind power periods, especially when the forecasted load is high. Thus, they would like information for the performance of the wpf tool taking into account the forecasted values.

To obtain such information, a classification of the forecasting errors according to the forecasted value, e.g. high, medium or low wind, is performed. For each forecasted value range, the wpf error pdf is derived and convoluted with $l_e(t)$ in order to derive the $lw_e(t)$ pdf, as well as the confidence intervals for the specific range of forecasted wind power, similar to Case 3. The approach here is based on the off-line evaluation and categorization of the results. Sometimes, the forecasting tool can provide pdf for the expected forecasting error according to the forecasted value using uncertainty estimations.

Economic Scheduling Functions

Equation (21) provides the minimum load that the units to be committed should meet, $Ld2Units(t)$, at each time interval t:

$$Ld2Units(t) = perc[q, lw_e(t)] + load(t) - WP(t) \tag{21}$$

The highest values of $F_{lwe(t)}[lw_e(t)]$ correspond to the overestimation of wind power and the underestimation of load, the case the system might be inadequate. Therefore, q is selected high (e.g. 98.5%), so that the risk of insufficient committed capacity is less than $1-q$ (e.g. 1.5%).

The unit commitment (UC) problem is solved next, to determine the status of each of the *unno* thermal units, using the following formulation for each time interval:

$$Min[OC(t)] = Min\left\{\sum_{i=1}^{unno}[u_{i,t} \cdot FC[Pg_i(t)] + u_{i,t} \cdot (1-u_{i,t-1}) \cdot SUC_i(t)]\right\} \tag{22}$$

where $OC(t)$ is the operating cost, $FC[Pg_i(t)]$ is the fuel cost (*FC*; quadratic cost function) of unit i depending on its production $Pg_i(t)$, $u_{i,t}$ is the unit status (0 if unit is off, 1 if unit is on). $SUC_i(t)$ denotes the start up cost of the ith unit that may be either constant, or a function of the time that the unit is not in operation, usually exponential.[30] In the power system studied, $SUC_i(t)$ is considered constant because switching concerns mainly fast start-up units.

The minimization of equation (22) is subject to the following constraints, for each time step:

$$\sum_{i=1}^{unno} u_{i,t} \cdot P_i^{max} \geq Ld2Units(t) \tag{23}$$

and

$$P_i^{min} \leq Pg_i(t) \leq P_t^{max} \tag{24}$$

where P_i^{min} and P_i^{max} are the technical minimum and maximum of unit i, respectively.

For the solution of the UC problem, the priority list is used. The units to be committed might impose constraints in the operation of the wind parks, i.e. underestimation of wind power and overestimation of the load means lower load to be dispatched. There might be the case that the sum of the technical minima of the units committed will be larger than the actual load to be served, as seen in equation (25):

$$\sum_{j \in IN(t)} P_j^{min} = load(t) - WP(t) + perc[p, lw_e(t)] \tag{25}$$

where $IN(t)$ is the set of the committed units and p is the value of the percentile, usually very small, e.g. $p = 1.5\%$, meaning that the probability of violating the technical minima is less than $p\%$. If inequality (25) is satisfied, then some wind power should be curtailed and the maximum acceptable wind power production, $WP(t)$, is given by equation (26):

$$WP(t) = load(t) + perc[p, lw_e(t)] - \sum_{j \in IN(t)} P_j^{min} \tag{26}$$

The set points of the committed units are finally calculated from the ED problem. This is formulated as the minimization of the FC in equation (27), meeting the load as described in equation (28), without violating the technical limits of the units in equation (24):

$$\min \sum_{j \in IN(t)} FC[Pg_j(t)] \tag{27}$$

$$\sum_{j \in IN(t)} Pg_j = load(t) - WP(t) \tag{28}$$

In order to solve the ED optimization problem, the sequential quadratic programming method is used. This is a generalization of the Newton's optimization method, which uses a quadratic approach of the non-linear objective function of *FC*s and linear approximations for the technical constraints. This method guarantees that the solution is the global optimum in the feasible space, if the objective function is convex.[31,32]

Study Case Network

General Description of the Power System

The case study network is the power system of Crete, which is the largest isolated system in Greece, with the highest annual increase in energy demand (8%). Various types of thermal units are in operation: steam turbines; diesel units; gas turbines; and one combined cycle plant. In the following, actual load and wind power time series for 2000 are used. The annual wind power penetration in energy is around 10%, whereas the instantaneous (hourly) wind power penetration has reached 39% in winter and early spring.[33]

The installed wind power capacity for the studied year is *InsCap* = 67.35 MW. Nowadays, the installed capacity is 105 MW, and the other 111.17 MW has been granted installation authorization from the Regulatory Authority of Energy in Greece.[34]

Technical Challenges Associated with Wind Power Forecasting

Wind power forecasting and estimation of its confidence interval are important during low-load and high-load periods. During low-load periods, there is a danger of low-loading operation of the base units (steam turbines and combined cycle unit), and wind power is curtailed to avoid violation of the technical minima. During high-load periods, overestimation of wind power may lead to insufficient power to meet the demand.

Selected Days for the Study

Nine representative days are considered (Table III), in order to study the impact of various levels of wind power production and demand. These days combine low, medium and high demand with low (LW), medium (MW) and high wind power production (HW). The considered characterization and the frequency of the respecting conditions are also presented in the same table. For each day, the actual time series for both load and wind power production—24 h at hourly steps—are used as inputs. The load time series are classified according to the daily demand as follows:

- High load (HL): above 6100 MWh, typically high touristic, summer days.
- Medium load (ML): between 5250 and 6100 MWh.
- Low load (LL): below 5250 MWh, typically during March, April, November and Sundays.

The wind power production time series are classified as follows:

- HW: above 40 MW for 75–80% of the day.
- MW: production between 17 and 40 MW for 75–80% of the day.
- LW: all the other available 24 h time series.

Table III. Typical days used

Day	Total daily demand (MWh)	Average wind power production (MW)	Characterization of day	Percentage within a year (%)
1	7269.8	55.2	HL–HW	11.75
2	7396.5	26.6	HL–MW	8.47
3	8006.1	7.5	HL–LW	9.56
4	5589.1	37.3	ML–HW	9.02
5	5421.1	24.1	ML–MW	11.75
6	5847.4	5.0	ML–LW	12.02
7	5242.7	40.7	LL–HW	4.64
8	4997.3	23.7	LL–MW	11.48
9	5197.4	1.3	LL–LW	21.31

From initial runs of the methodology for many other days meeting the same criteria with the nine representative days of Table III, neither the sign of the cost difference nor the relative difference of wind power curtailment among the assumed information levels of Table I has changed. That is why the results presented in this paper focus on the nine representative days of Table III.

Forecasting Tool Characteristics

In this paper, the *NMAE* of the MORE CARE load and wind power forecasting functions for 24 h ahead, as applied in Crete, are used[7]. These functions employ fuzzy-neural techniques for load forecasting and fuzzy-neural network coupled with meteorological information for wind power forecasting. *NMAE* values for both forecasting tools are given in Table IV.

For load forecasting, the frequency of overestimation and underestimation errors is assumed equal, i.e. $a = b = 50\%$. For wind power forecasting, Table II presents:

• The selected values for the occurrence of underestimation and overestimation errors.
• The calculated NBIAS and standard deviation corresponding to the selected values.

It should be noted that 97% confidence interval was considered in Table II and the corresponding k_q and k_p parameters are equal to 2.17.

For the other two cases, the distribution of wpf errors has been considered either as it is for Case 3, or after grouping these errors according to the wind power output, Case 4. The forecasting errors have been obtained from the evaluation of the MORE CARE forecasting tool with actual data for 1 year.[24]

Results and Discussion

Overview

The presented results focus on the change in the operating cost and the expected wind power curtailment for each day of Table III according to the wpf error information available. The results show that the actual energy produced by the thermal units is almost the same in all studied cases, but two parameters differentiate costs:

• The number and the type of units committed to meet the same demand.
• The amount of wind power curtailment that modifies the energy dispatched to the thermal units. The higher the wind power curtailment, the higher the increase in thermal production and cost.

Impact of Wind Power Forecasting Error Bias on Wind Power Curtailment

Assuming the same *NMAE* for all cases, the different values for wpf NBIAS in Table II are compared with respect to wind power curtailment and operating cost.

Figure 4 shows the absolute values of wind power curtailment during days with MW or HW, and LL or ML plotted for different values of frequency of wind power underestimation. Wind power curtailment is sensitive to:

• Variation of load, as shown by comparing days with the same level of wind power production but different load level, e.g. LL–HW with ML–HW day. For the same level of wind power underestimation frequency, wind power curtailment for LL–HW is higher than for ML–HW day.

Table IV. *NMAE* forecasting errors for load and wind power

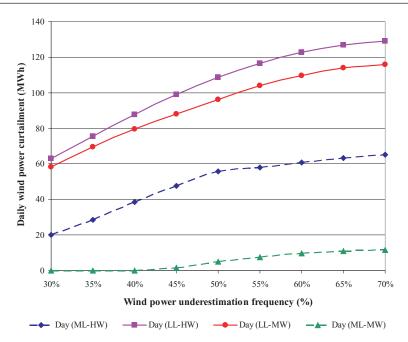|	
Load forecasting (*NMAE*$_l$)	7.07%
Wind power forecasting (*NMAE*$_w$)	14.06%

Figure 4. Absolute values of daily wind power curtailment versus wind power underestimation frequency for high and medium wind periods
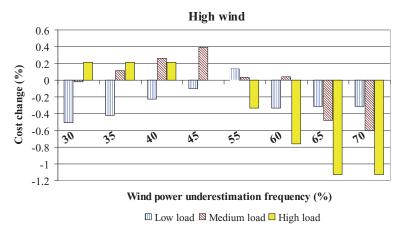

Figure 5. Cost comparison for high wind production for different wind power underestimation frequency

- Variation of wind power production, as shown by comparing days with similar loading but different wind power production, e.g. LL–HW and LL–MW days. For the same level of wind power underestimation frequency, wind power curtailment for LL–HW is higher than for LL–MW day.
- Variation of frequency of wind power underestimation. For the same day type (e.g. ML–HW), wind power curtailment is increased as the wind power underestimation frequency increases.

Impact of Different Wind Power Forecasting Bias Values on Cost

The economic impact of different bias on the wpf error is studied in this section. Positive values of cost difference (Figures 5–7) denote rise, whereas negative values denote decrease in the operating cost compared with
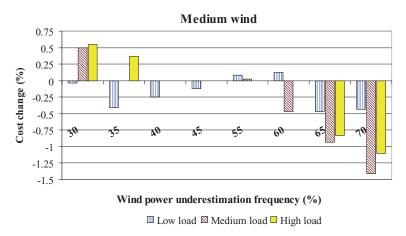
Figure 6. *Cost comparison for medium wind production for different wind power underestimation frequency*
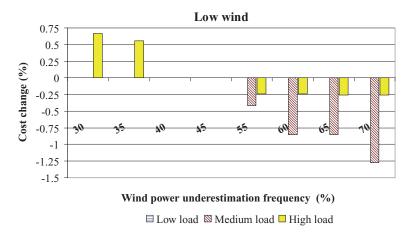

Figure 7. *Cost comparison for low wind production for different wind power underestimation frequency*

the base case (Case 1). The results are grouped into high, medium and low wind periods, compared for each case individually with different demands and with different frequencies of wind power underestimation.

For HW days (Figure 5), for high-demand periods, the operating cost is decreased as the frequency of wind power underestimation increases because of reduced spinning reserve requirements. Cost reduction is equal for some neighboring values of the frequency of wind power underestimation (i.e. 30, 35 and 40 %) because of the commitment of the same units without wind power curtailment. For medium demand periods, when the frequency of wind power underestimation is below 50%, the operating cost is increased as the frequency of wind power underestimation increases, because of wind power curtailment (Figure 4). This justifies the lower cost increase for 40% compared with 45%, and the marginal cost increase for 55 and 60% frequency of wind power underestimation. For all these cases, there is no difference in the committed units but wind power curtailment increases thermal production and thus operating costs.

Similar conclusions hold for MW days (Figure 6) as for HW days (Figure 5).

In LW days (Figure 7), wind power is not curtailed, so the cost is affected only by the thermal operation. For ML days, operating-cost change exists only for wind power underestimation above 50%. No operating-cost change is noted for any value for LL days, as the low wind power production has minor impact on the operation of base or intermediate loading.

Impact of Increased Information on Wind Power Forecasting Error

Following the comparison of the impact of different frequencies of wind power underestimation, which is equivalent to different NBIAS values when Normal pdf for wpf error is assumed, the impact of different information level on the performance of the same wpf tool is studied. The four cases of Table I are compared and the impacts on wind power curtailment and operating cost are studied.

Figure 8 shows the estimated wind power curtailment for the days and cases studied. The days and cases not depicted present zero wind power curtailment. Figure 8 shows that in all these cases, during high wind periods and ML or LL, there is significant wind power curtailment. For similar daily wind power production, wind power curtailment is increased as load decreases, as shown by the comparison of LL–MW with ML–MW or LL–HW with ML–HW days.

Case 3 presents the highest wind power curtailment for all the days studied except for the LL–LW day for which Case 4 presents the highest value. The increased wind power curtailment in Case 3 is justified by the distribution of wpf underestimation errors (Figure 3), which is not actually a Normal distribution around NBIAS, but presents—much more often than the corresponding Normal pdf assumed for Case 2—significant values of wind power underestimation error. This fact justifies the relatively small but existing wind power curtailment noted for an LL–LW day.

For HW periods, Case 4 leads to the lowest wind power curtailment compared with all the other cases, as LL–HW and ML–HW days show (Figure 8). For high wind periods, the probability to underestimate the forecasted wind power is significantly lower. This fact is not taken into account when considering common wpf error distribution for all forecasted values, as Case 3 does, or even worse, when a Normal pdf is assumed like Cases 1 and 2. On the contrary, for low wind periods, it is more probable that the wind power is underestimated by the wpf tool, leading to increased uncertainty about the low limit of the expected load to be served by the committed thermal units. This is visible in Figure 8, when during low demand, even with low wind about 10 MWh wind power is curtailed, the highest among the cases studied.

For MW periods, wind power curtailment for Case 4 is higher, than the wind power curtailment for Cases 1 and 2. This is explained as the possibility of rather increased wind power underestimation is higher compared with the hypothesis of Normal pdf. Nevertheless, such a probability is considerably lower than the one for Case 3, which presents higher wind power curtailment compared with Case 4. It is also notable that wind power curtailment for Case 4 is almost equal for the 2 days (ML–MW and ML–HW), showing the impact of the detailed analysis of the wpf error according to classified prediction outputs.

The wind power curtailment analysis shows that the exact distribution of wpf errors independently of the forecasted value, Case 3, neither identifies the high possibility of wind power curtailment during the low wind
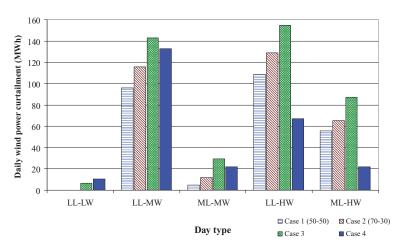

Figure 8. Wind power curtailment for different types of days for the studied cases

days, nor the lower possibility of wind power curtailment during medium or even higher wind periods. Cases 1 and 2, assuming very low probability for high wind power underestimation value, failed to estimate the requirement for wind power curtailment during the periods suggested by Cases 3 and 4.

Cost Comparison

Comparing Cases 3 and 4 to Cases 1 and 2

The economic impact of increased information about the performance of the wpf tool is studied in this section. First, Case 1 is compared with Cases 3 and 4 (Figure 9), and then Case 2 (representing the performance of the forecasting tool) is compared with Cases 3 and 4 (Figure 10). In both figures, results are presented in ascending order of demand, grouped for each level of wind power forecast, namely, low, medium and high.

Comparing 50% and 70% frequency of wind power underestimation is equivalent to the comparison of Case 1 and Case 2, respectively. In all cases, Case 2 presents equal or lower costs than Case 1. This cost reduction is low for low wind periods, but can reach up to 1.41% for an ML–MW day.

Low cost increase is noted only for an LL–LW day, when Case 3 is compared with Case 1 (Figure 9). As the operating units in both Cases 1 and 3 are the same, this is because of increased wind power curtailment. For all the other studied days, there is significant cost decrease when comparing Case 3 with Case 1. This cost decrease is justified by the fact that not only Case 3 presents the same average frequency of wind power underestimation with Case 2, higher than Case 1, but also presents more often higher wind power underestimation values than the Normal pdf assumption. Thus, the spinning reserve requirements for Case 3 are significantly reduced compared with Case 1.

If one compares Cases 2 and 3 (Figure 10), cost decrease exists in all days studied, with the exception of the LL–LW day justified by the wind power curtailment. The wind power curtailment difference between Cases 2 and 3 is significantly lower compared with the difference between Cases 1 and 3. Thus, the impact of wind power curtailment in the cost difference shown in Figure 10 compared with the one of Figure 9 is alleviated. The difference in spinning reserve requirements for Cases 2 and 3 is lower than between Cases 1 and 3, and consequently the cost reduction for Case 3 is significantly lower in Figure 10 compared with Figure 9. Nevertheless, reduction of operating cost in Case 3 is still noted compared with Case 2, as high values of overestimating the forecasted wind power are less frequent than the ones foreseen using the Normal pdf.
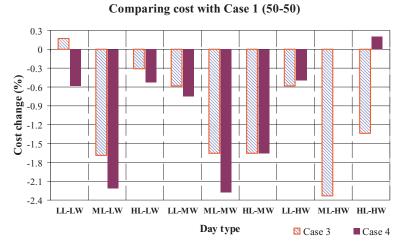

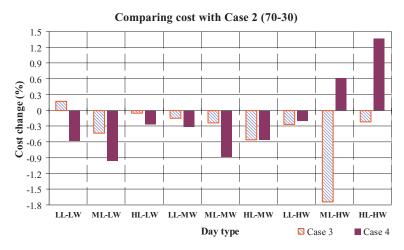Figure 9. Cost comparison of Case 1 with Cases 3 and 4

Figure 10. Cost comparison of Case 2 with Cases 3 and 4

The comparison between Case 2 and Case 4 (Figure 10) versus Case 1 and Case 4 (Figure 9) presents lower cost difference in both absolute and percentage values regarding low or medium wind power production. The lower spinning reserve requirements for Case 2 compared with Case 1 reduces the difference in spinning reserve requirements between Cases 2 and 4, and thus the operating costs difference.

Conclusion

In this paper, a method based on probabilistic analysis is presented that exploits any available information about load and wind power forecasting errors, to derive user-defined percentiles of the error in the estimation of the load to be distributed to the thermal units of an autonomous power system. These percentiles form confidence intervals that can be used not only to calculate the spinning reserve requirements, but also to estimate the possibility of thermal units' technical minima violation. The methodology developed here can be also applied for interconnected power systems, if constraints for the interconnection lines are considered.

The economic impact of various levels of information on the wpf error has been evaluated using actual data and an applied wpf tool, showing significant changes in both operating costs and wind power curtailment. It has been also shown that for autonomous power systems, high underestimation errors may lead to increased wind power curtailment to avoid co-operation of thermal units with wind power.

The analysis has shown that, even by off-line classification of the wpf errors according to the forecasted values, the operators may find that overestimation of wind power production for low and medium wind periods is less important than for high wind periods. Therefore, information about the uncertainty of wpf output in the form of confidence intervals for different forecasting levels can aid operators to estimate the expected range of wind power production and, consequently, the expected range of the load to be dispatched to the thermal units. The methodology can exploit any information on forecasting errors. Such information may be either a pdf of the expected forecasting error provided by the forecasting tool itself, or a pdf extracted from off-line evaluation of the forecasting tools.

Acknowledgements

Appendix

In the following, the transformation of equation (6) into equation (8) is presented.

$$\int_{-\infty}^{\infty} |e_r| \cdot N(e_r, \mu_e, \sigma) \cdot de_r = NMAE \Rightarrow$$

$$\int_{-\infty}^{\infty} |e_r| \cdot \frac{1}{\sigma \cdot \sqrt{2 \cdot \pi}} \cdot \exp\left(-\frac{1}{2} \cdot \left(\frac{e_r - \mu_e}{\sigma}\right)^2\right) \cdot de_r = NMAE \Rightarrow$$

$$-\int_{-\infty}^{0} e_r \cdot \frac{1}{\sigma \cdot \sqrt{2 \cdot \pi}} \cdot \exp\left(-\frac{1}{2} \cdot \left(\frac{e_r - \mu_e}{\sigma}\right)^2\right) \cdot de_r + \int_{0}^{\infty} e_r \cdot \frac{1}{\sigma \cdot \sqrt{2 \cdot \pi}} \cdot \exp\left(-\frac{1}{2} \cdot \left(\frac{e_r - \mu_e}{\sigma}\right)^2\right) \cdot de_r = NAME \Rightarrow \tag{29}$$

$$\frac{\sigma}{\sqrt{2 \cdot \pi}} \cdot \int_{-\infty}^{0} -\frac{(e_r - \mu_e)}{\sigma^2} \cdot \exp\left(-\frac{1}{2} \cdot \left(\frac{e_r - \mu_e}{\sigma}\right)^2\right) \cdot de_r - \mu_e \cdot \int_{-\infty}^{0} \frac{1}{\sigma \cdot \sqrt{2 \cdot \pi}} \cdot \exp\left(-\frac{1}{2} \cdot \left(\frac{e_r - \mu_e}{\sigma}\right)^2\right) \cdot de_r +$$

$$\mu_e \cdot \int_{0}^{\infty} \frac{1}{\sigma \cdot \sqrt{2 \cdot \pi}} \cdot \exp\left(-\frac{1}{2} \cdot \left(\frac{e_r - \mu_e}{\sigma}\right)^2\right) \cdot de_r - \frac{\sigma}{\sqrt{2 \cdot \pi}} \cdot \int_{0}^{\infty} -\frac{(e_r - \mu_e)}{\sigma^2} \cdot \exp\left(-\frac{1}{2} \cdot \left(\frac{e_r - \mu_e}{\sigma}\right)^2\right) \cdot de_r = NMAE$$

Taking into account that:

$$\int_{-\infty}^{0} \frac{1}{\sigma \cdot \sqrt{2 \cdot \pi}} \cdot \exp\left[-\frac{1}{2} \cdot \left(\frac{e_r - \mu_e}{\sigma}\right)^2\right] \cdot de_r = a \tag{30}$$

$$\int_{0}^{\infty} \frac{1}{\sigma \cdot \sqrt{2 \cdot \pi}} \cdot \exp\left[-\frac{1}{2} \cdot \left(\frac{e_r - \mu_e}{\sigma}\right)^2\right] \cdot de_r = b \tag{31}$$

$$\int_{-\infty}^{0} -\frac{(e_r - \mu_e)}{\sigma^2} \cdot \exp\left[-\frac{1}{2} \cdot \left(\frac{e_r - \mu_e}{\sigma}\right)^2\right] \cdot de_r = \exp\left[-\frac{1}{2} \cdot \left(\frac{-\mu_e}{\sigma}\right)^2\right] \tag{32}$$

$$\int_{0}^{\infty} -\frac{(e_r - \mu_e)}{\sigma^2} \cdot \exp\left[-\frac{1}{2} \cdot \left(\frac{e_r - \mu_e}{\sigma}\right)^2\right] \cdot de_r = \exp\left[-\frac{1}{2} \cdot \left(\frac{-\mu_e}{\sigma}\right)^2\right] \tag{33}$$

By using equation (30) to (33), equation (29) is transformed into equation (8), that is

$$\mu_e \cdot (b - a) + 2 \cdot \frac{\sigma}{\sqrt{2\pi}} \cdot \exp\left[-\frac{1}{2} \cdot \left(-\frac{\mu_e}{\sigma}\right)^2\right] = NMAE \tag{8}$$

References

1. Landberg L, Giebel G, Nielsen HA, Nielsen TS, Madsen H. Short-term prediction—an overview. *Wind Energy* 2003; **6**: 273–280.
2. Giebel G, Brownsword R, Kariniotakis G. The state-of-the-art in short-term prediction of wind power: a literature overview. [Online]. Available: http://anemos.cma.fr/download/ANEMOS_D1.1_StateOfTheArt_v1.1.pdf. (Accessed 12 July 2007)
3. Bremnes JB. A comparison of a few statistical models for making quantile wind power forecasts. *Wind Energy* 2006; **9**: 3–11.
4. Ackermann, T. *Wind Power in Power Systems*. John Wiley & Sons: Chichester, England, 2005.
5. Bremnes JB. Probabilistic wind power forecasts using local quantile regression, *Wind Energy*. 2004; **7**: 47–54.
6. Sideratos G, Hatziargyriou N. An advanced statistical method for wind power forecasting. *IEEE Transactions on Power Systems* 2007; **22**: 258–265.
7. Kariniotakis G, Mayer D, Halliday JA, Dutton AG, Irving AD, Brownsword RA, Dokopoulos P, Alexiadis M. Load, wind and hydro power forecasting functions of the More-Care EMS system. *Proceedings of MedPower Conference*, Athens, Greece, November 2002, Paper MED02/003.

8. Hatziargyriou N, Contaxis G, Atsaves G, Matos M, Pecas Lopes JA, Vasconcelos MH, Kariniotakis G, Mayer D, Halliday JA, Dutton AG, Dokopoulos P, Bakirtzis A, Stefanakis J, Gigantidou A, O'Donell P, McCoy D, Costello R, Fernandes MJ, Cotrim JMS, Figueira AP. MORE CARE overview. *Proceedings of MedPower Conference*, Athens, Greece, November 2002, Paper MED02/002.

9. Hatziargyriou N, Tsikalakis AG, Dimeas A, Georgiadis D, Gigantidou A, Stefanakis J, Thalassinakis E. Security and economic impacts of high wind power penetration in island systems. *Proceedings of Cigre Conference*, Paris, France, August 2004.

10. Milligan MR, Miller AH, Chapman F. Estimating the economic value of wind forecasting to utilities. *Proceedings of Windpower Conference*, Washington DC, March 1995, Paper NREL/TP-441-7803. [Online]. Available: http://www.nrel.gov/docs/legosti/old/7803.pdf (Accessed 12 July 2007)

11. Parsons B, Milligan M, Zavadil B, Brooks D, Kirby B, Dragoon K, Caldwell J. Grid impacts of wind power: a summary of recent studies in the United States. *Wind Energy* 2004; **7**: 87–108.

12. Gilman B, Cheng M, Isacc J, Zack J, Bailey B, Brower M. The value of wind forecasting to Southern California Edison. *Proceedings of WindPower Conference*, USA, June 2001, Paper 021.

13. Usaola J, Ravelo O, González G, Soto F, Carmen Dávila M, Díaz–Guerra B. Benefits for wind energy in electricity markets from using short term wind power prediction tools; a simulation study. *Wind Engineering* 2004; **28**: 119–128.

14. ANEMOS Project. Wind prediction in electricity markets. ANEMOS Project, Deliverable D8.2. [Online]. Available: http://anemos.cma.fr/. (Accessed 12 July 2007)

15. Pinson P, Nielsen H, Møller J, Madsen H, Kariniotakis G. Non-parametric probabilistic forecasts of wind power: required properties and evaluation. *Wind Energy* 2007; **10**:497–516.

16. Nielsen HA, Nielsen TS, Madsen H, Sattler K. Wind power ensemble forecasting. *Proceedings of the Global Wind Power Conference*, Chicago, IL, 2004.

17. Nielsen HAa, Nielsen TS, Madsen H, Badger J, Giebel G, Landberg L, Sattler K, Voulund L, Tøfting J. From wind ensembles to probabilistic information about future wind power production—Results from an actual application. *Proceedings of the PMAPS Conference*, Stockholm, Sweden, 2006.

18. Lange M, Focken U. *Physical Approach to Short-term Wind Power Prediction*. Berlin: Springer Verlag, 2005.

19. Gneiting T, Larson K, Westrick K, Genton MG, Aldrich E. Calibrated probabilistic forecasting at the stateline wind energy center—the regime-switching space-time method. *Journal of the American Statistical Association* 2006; **101**: 968–979.

20. Nielsen HAa, Madsen H, Nielsen TS. Using quantile regression to extend an existing wind power forecasting system with probabilistic forecasts. *Wind Energy* 2006; **9**: 95–108.

21. Pinson P. Estimation of the uncertainty in wind power forecasting. PhD Dissertation, Ecole des Mines de Paris, 2006. [Online]. Available: www.imm.dtu.dk/pp. www.pastel.paristech.org/bib. (Accessed 11 May 2007)

22. Pinson P, Chevallier C, Kariniotakis G. Optimizing benefits from wind power participation in electricity markets using wind power forecasting embedded with uncertainty management tools. *Proceedings of European Wind Energy Conference*, London, UK, November 2004.

23. Pinson P, Kariniotakis G. On-line assessment of prediction risk for wind power production forecasts. *Wind Energy* 2004; **7**: 119–132.

24. Hatziargyriou N, Dimeas A, Tsikalakis A, Gigantidou A, Thalassinakis E. Intelligent techniques applied to the economic and secure operation of island systems with large wind power penetration. *Proceedings 2003 ISAP Conference*, Lemnos, Greece, September 2003, paper ISAP 03/162.

25. Madsen H, Pinson P, Kariniotakis G, Nielsen HA, Nielsen TS. Standardizing the performance evaluation of short-term wind power prediction models. *Wind Engineering* 2005; **29**: 475–489.

26. Papoulis A. *Probability and Statistics.*Prentice Hall: Englewood Cliffs, NJ, 1990.

27. Miranda V, Cerqueira C, Monteiro C. Training a FIS with EPSO under a entropy criterion for wind power prediction. *Proceedings of the 9th International Conference of Probabilistic Methods Applied to Power Systems*, Stockholm, Sweden, 11–15 June 2006.

28. Lange M. Analysis of the uncertainty of wind power predictions. PhD Thesis, Carl von Ossietzky University, Oldenburg, Germany, 2003.

29. Saint-Drenan, YM. Wind power predictions analysis. Part. 2: economical analysis. *ECN-I–02-011*; August, 2002. [Online]. Available: http://www.ecn.nl/docs/library/report/2002/i02011.pdf. (Accessed 12 July 2007).

30. Momoh JA. *Electric Power System Applications of Optimization*. Marcel Dekker: New York, 2001.

31. Han XS, Gooi HB, Kirschen DS. Dynamic economic dispatch: feasible and optimal solutions. *IEEE Transactions on Power Systems* 2001; **16**: 22–28.

32. Rao SS. *Engineering Optimization: Theory and Practice* (3rd edn). John Willey & Sons: New York, 1996.

33. Stefanakis J. Crete: An ideal case study for increased wind power penetration in medium sized autonomous power systems. *Proceedings of IEEE PES Winter Meeting*, 2002; 329–334.

34. Hatziargyriou N, Tsikalakis A, Androutsos A. Status of distributed generation in Greek islands. *Proceedings of IEEE PES General Meeting*, Montreal, Canada, June 2006, Paper 06GM0368.